Electronic and optical properties of Si/SiO_2 nanostructures. II. Electron-hole recombination at the Si/SiO_2 quantum-well–quantum-dot transition

N. Pauc,[1,*] V. Calvo,[1,†] J. Eymery,[1] F. Fournel,[2] and N. Magnea[1]
[1]*CEA Grenoble, DRFMC/SP2M/SiNaPS, 17 rue des Martyrs, 38054 Grenoble Cedex 9, France*
[2]*CEA-DRT-LETI, CEA/GRE, 17 rue des Martyrs, 38054 Grenoble Cedex 9, France*
(Received 3 June 2005; published 18 November 2005)

A photoluminescence (PL) study of crystalline Si/SiO_2 quantum wells has been carried out for thicknesses in the 3.9–0.6 nm range. We show that quantum confinement plays a great role on emission properties of these narrow quantum wells in term of PL line energy and quantum efficiency. In particular, for the very-low-thickness domain, a set of discrete and high-energy lines is observed between 1.20 and 1.60 eV and viewed as resulting from two phenomena: the thickness fluctuations of the silicon layer and the appearance of structural barriers in the plane of the thinnest wells due to the formation of a two-dimensional distribution of Si nanocrystals embedded in SiO_2. A strong increase in the photoluminescence efficiency is measured for wells pertaining to the very-low-thickness domain.

DOI: 10.1103/PhysRevB.72.205325 PACS number(s): 73.21.Fg, 78.55.−m, 78.67.De, 05.30.Fk

I. INTRODUCTION

In the last few years, intense research has been performed in the field of crystalline silicon (*c*-Si) based light emitting devices. Despite the very poor internal quantum efficiency (QE) of this material (of the order of 1×10^{-5}), several ways for the enhancement of the *c*-Si external luminescence have been explored. Recombination of electron-hole (e-h) pairs in implanted bulk *c*-Si at room temperature with high efficiency[1] or strong spatial localization of carriers leading to an increase of direct recombination in silicon crystallites[2] are promising techniques for the realization of efficient *c*-Si optical sources. The exceptional room-temperature photoluminescence (PL) properties of this class of material were discovered by Canham in 1990 (Ref. 3) in porous silicon obtained by electrochemical etching. This discovery involved a great number of studies concerning silicon nanocrystals (*nc*-Si) (Ref. 4) whose size and density control is of outstanding importance for optical or electronic applications. While many works were focused on the optical properties of very thin Si/SiO_2 quantum wells (QW's) obtained by thinning of silicon-on-insulator (SOI) substrates fabricated by the separation by the implanted oxygen technique (SIMOX),[5–9] no detailed study was performed to highlight the connections and transition between ultrathin *c*-Si QW's and *nc*-Si.

In a previous article,[10] we showed that quantum confinement played an important role in the photoluminescence properties of the two-dimensional electron-hole liquid (EHL) in optically pumped Si/SiO_2 QW's for thickness l_z below $3a_x$, where $a_x\approx4.9$ nm is the bulk exciton Bohr radius. However, no result was presented for $l_z<a_x$ where the QW thickness becomes comparable to the diameter of *nc*-Si. The aim of this paper is to study such very confined electron-hole systems and to complete the work accomplished in thick *c*-Si QW's by a systematic study of the influence of the thickness decrease on the recombination spectra in the low-thickness domain (i.e., $l_z<4.7$ nm). A strong quantum confinement effect is observed in this l_z range, in analogy with the weak confinement effect[10] observed above $l_z\approx5$ nm. This results in a set of fixed high-energy lines in PL spectra. The data will be compared with a simple model which gives a direct connection between the line position and the QW thickness. For the sake of a greater physical significance, some improvement is brought by including the effect of the image charges in the dielectric barriers on the optical properties of thin *c*-Si QW's. It will be seen that thinning SOI substrates down to the length scale of the exciton Bohr radius appears as a promising and alternative way for the fabrication of SiO_2-embedded *nc*-Si.

II. SAMPLES AND EXPERIMENT

Samples are obtained from an initial 4-in. SOI wafer made using wafer bonding technology for the transfer of the standard 200-nm *c*-Si layer over the 400-nm thermal SiO_2/c-Si substrate stack. The upper SiO_2 barrier necessary to passivate the silicon surface is fabricated by thermal oxidation of the *c*-Si layer. Adjusting the oxidized amount of the *c*-Si layer following several oxidation-deoxidation cycles allows us to reach the desired silicon and upper oxide thicknesses—in our case 10 nm for both materials. Using spectroscopic ellipsometry, we noticed that wafer edges exhibited interesting zones with a silicon thickness gradient of the order of 1 nm per mm along the sample surface. These border zones are generally not processed in standard technology because of the edge effects. The accuracy of the ellipsometric measurements has been found to be ±0.5 nm. Setting the l_z dependence as a function of the position on the sample surface by means of this technique allows us to establish a one-to-one relation between PL spectra and the QW thickness.

Samples were immersed in a continuous gaseous helium flux at 6 K in the cryostat. Excitation was ensured by a $\lambda=351$ nm cw beam from an Ar^+ laser focused on the sample surface with a diameter of the order of 50 μm. The laser density power reached 4 kW cm^{-2}. Use of this particular wavelength is necessary for efficient excitation of *c*-Si nano-

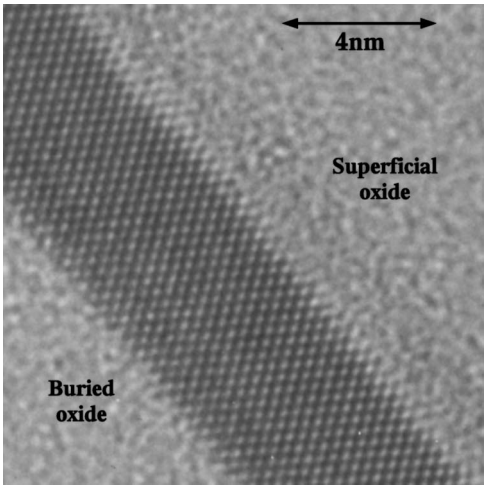

FIG. 1. Cross section of a SOI QW obtained after several cycles of oxidation and sacrificial deoxidation of Si. Each point corresponds to two unresolved atomic columns.

structures because it provides a strong absorption A in the direct gap of the material following the law $A(l_z)=1-\exp[-\alpha l_z]$, where $\alpha=9\times10^5$ cm^{-1} at $\lambda=351$ nm. We registered the reference spectrum of our 640-mm monochromator and photomultiplier tube with a cooled InGaAs photocathode to a white lamp (3400 K blackbody). We used it as a correction function for our broadband PL spectra to ensure better line-shape analysis.

III. PHOTOLUMINESCENCE OF SUB-4-nm Si/SiO$_2$ QUANTUM WELLS: STRONG QUANTUM CONFINEMENT REGIME

A. Effect of the thickness lowering

In a previous article,[10] we showed that lowering the *c*-Si QW thickness leads to a weak quantum confinement effect below $l_z\approx3a_x^{3D}$ and to a blueshift of the EHL line. However, no PL data were reported for QW's below $l_z\approx a_x^{3D}$, when carrier confinement is expected to play a crucial role in luminescence properties. The observed thickness gradients on wafer edges are particularly suitable for l_z-dependent PL studies and make possible a comparison between thicker QW's (Ref. 10) at high l_z and SiO_2 embedded *nc*-Si at low l_z.

The structural study of a narrow QW using transmission electron microscopy (TEM), as reported in Fig. 1, shows unambiguously that the crystalline quality of the *c*-Si QW is not altered by the various oxidation-deoxidation cycles necessary to reach the nominal thickness (10 nm). The Si/SiO_2 interface is defined at the atomic scale along the two QW sides, as for standard SOI substrates ($l_z=200$ nm). Thinning commercial SOI wafers using thermal oxidation appears as a promising technique to furnish high-quality *c*-Si QW's over a wide range of thickness, from 200 nm down to a few nanometers—the crystalline quality of thinner layers (about 1 nm) has also been checked at the European Synchrotron Radiation Facility (ESRF) by grazing-incidence x-ray diffraction. This method is particularly interesting in view of the "classical" epitaxial Si/SiGe technique which provides

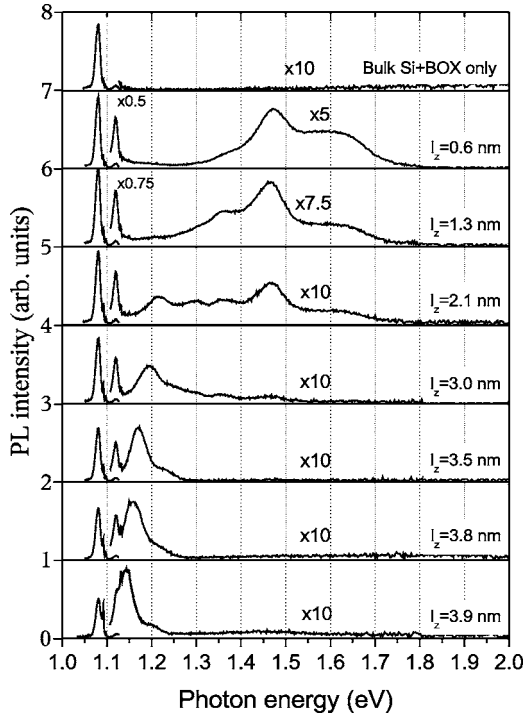

FIG. 2. Well PL as a function of l_z in a variable thickness QW (ellipsometric measurements of l_z label each spectra). Laser density power is $\mathcal{P}=4$ kW cm^{-2} and $T\approx6$ K. All spectra have been corrected from the setup response to the 3400 blackbody.

c-Si QW's with finite-height barriers and weak carrier confinement.

PL spectra acquired at $\mathcal{P}=4$ kW cm^{-2} and $T=6$ K with a focused laser beam are reported in Fig. 2. In the experimental setup, the sample is free to move in the perpendicular plane to the focused laser beam. Control of lateral movements thanks to a micrometric translation stage makes possible l_z-dependent studies of QW PL by tuning the sample position with respect to the laser beam along the thickness gradient. From Fig. 2, one can see that spectra can be divided into several groups. The first group contains a fixed set of lines on the low-energy side of the PL spectra for any position of the laser spot or any analyzed thickness. These lines are found to be the TO-LO EHL and bound-exciton (BE) phonon replica centered at 1.082 and 1.092 eV and also the corresponding TA replica at 1.120 and 1.132 eV, and arise from e-h recombination in the substrate.[11] The second kind of luminescence line is observed at high energy for l_z between 3.9 and 2.1 nm. As for the two-dimensional (2D) EHL identified in Ref. 10, this "moving" line blueshifts as l_z decreases. Fits of the EHL line maximum E_M deduced from spectra in Fig. 1 of Ref. 10 for $l_z\geqslant4.7$ nm give the empirical relation $E_M(\text{meV})\approx1081+1105/l_z^2$. When compared to the experimental maximum $E_M=1145$ meV of the $l_z=3.9$ nm spectrum in Fig. 2, one obtains the extrapolated thickness $l_z^e\approx4.16$ nm, which is very close to the ellipsometric measurements. We conclude that the moving line observed in spectra of Fig. 2 down to $l_z=2.1$ nm is ascribed to e-h recombination via confined electronic states.

Below $l_z\approx2.1$ nm, a new series of fixed and discrete high-energy lines arises in the e-h recombination spectra.

Such spectra cannot be due to a wavelength-dependent sensitivity of our experimental setup since spectra recorded in Fig. 2 have been divided by the setup response to the 3400 K blackbody light, assumed to be a white light in the spectral interval of acquisition.

In order to determine the origin of the observed high-energy radiations, we etched the superficial oxide and silicon layers of a similar sample using a buffered HF solution and an aqueous TMAH solution. The spectrum of the resulting structure (bulk *c*-Si substrate+buried oxide) is reported in the top of Fig. 2 and only exhibits e-h recombination in the substrate under the same pumping and temperature conditions than for the other reported spectra. This shows unambiguously that light emission occurs in the *c*-Si QW and/or at the Si/SiO_2 interface.

Spectra acquired for $l_z \leqslant 2.1$ nm have been fitted using five Gaussian curves. Results indicate that the e-h recombination line positions[12] are constant for all spectra (similar behaviors have been found in other samples) with values $E_{M1}=1.21$ eV, $E_{M2}=1.29$ eV, $E_{M3}=1.36$ eV, $E_{M4}=1.46$ eV, and $E_{M5}=1.60$ eV. As no line was observed in the spectral range between 1.60 eV and the upper cutoff of the detector sensitivity—determined to be above 3 eV—it is likely that no more energetic line appears beyond the fifth component.

In view of these results, we shall give a very simple description of the electronic processes that can explain the shape of the spectra in Fig. 2 as resulting from e-h recombination via highly confined electronic states in Si/SiO_2 nanostructures. The EHL line blueshift observed below $l_z \approx 3a_x$ in Fig. 1 of Ref. 10 is well explained in thin QW's by both an opening of the band gap and a rigid band shift due to many-body phenomena given, respectively, by *ab initio* calculations of the *c*-Si band diagram from Niquet *et al.*[13] and the adapted theory of Kleinman.[14] More precisely, the line position depends on a quantum confinement term $E_{Qc}=E_c-E_v$ and on a Coulomb term E_{Cb} taking account of the image charge effect. Following Ref. 13, we have

$$E_v(l_z) = \frac{K_v}{l_z^2 + a_v l_z + b_v}, \tag{1}$$

$$E_c(l_z) = \frac{K_c}{l_z^2 + a_c l_z + b_c} + E_g, \tag{2}$$

where l_z is in nm, $K_v=-1326.2$ meV nm^2, $a_v=1.418$ nm, $b_v=0.296$ nm^2, $K_c=394.5$ meV nm^2, $a_c=0.939$ nm, and $b_c=0.324$ nm^2. The negative E_{Cb} term arises from many-body interactions inside the plasma. Here, for the sake of simplicity, we shall assume that E_{Cb} can be approximated by the exciton binding energy given by the Keldysh theory of excitons in semiconductor-dielectric nanostructures[15] including image charge effects. Finally, we have

$$\begin{aligned} E_M(l_z) &= E_{Qc}(l_z) + E_{Cb}(l_z) - \hbar\omega_{TO} \\ &= E_c(l_z) - E_v(l_z) - B_{EX}(l_z) - \hbar\omega_{TO}, \end{aligned} \tag{3}$$

with $B_{EX}(l_z)$ the thickness-dependent exciton binding energy given by Eq. (24) of Ref. 15. In Eq. (3), we assume that e-h recombination is assisted by constant-energy phonons in the range of studied l_z.

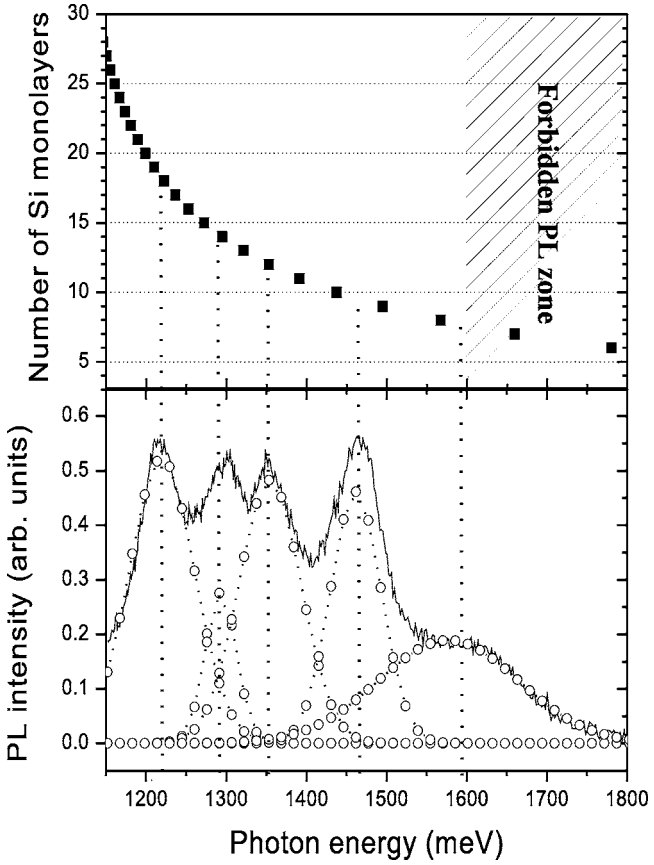

FIG. 3. Solid curve: PL spectra of the 2.1-nm QW (see Fig. 2). Circles: fit of the spectrum using a five-Gaussian curve set.

Thickness can be expressed in units of silicon monolayers η as $l_z=\eta a_{Si}/4$, where $a_{Si}\approx 0.5431$ nm is the silicon lattice constant. To compare our model with data, we selected the 2.1-nm QW PL spectrum with well-defined spectral components as shown in Fig. 3. Each Gaussian contribution (circles) is well separated from one another. Using Eq. (3) and measuring the experimental E_M allows us to estimate the corresponding η parameters. We find $\eta=19$, 14, 12, 10, and 8 monolayers for $E_M=1.21$, 1.29, 1.36, 1.46, and 1.60 eV, respectively.

In view of the observed spectra, some correlation emerges between η and the measured thickness along the Si gradient of the QW (see insets in Fig. 2). If we look at the general shape of the 1.3-nm spectrum reported in Fig. 2, we can note that the main contribution is centered at $E_M^4=1.46$ eV, with $\eta=10$. This leads to estimate the thickness obtained in the model of strong quantum confinement and gives $l_z \approx 1.36$ nm, in very good agreement with ellipsometric measurements. We conclude that the experimental spectra obtained in very narrow QW's are well explained in the framework of our model of carrier recombination under strong quantum confinement. Moreover, the characteristic form of the η series gives interesting data on the shape of the silicon gradient. One can see that two consecutive PL lines correspond to two distinct thicknesses with a mean separation of $\eta=2$ monolayers. This suggests to us that the Si gradient is made of terraces and steps with quantized thickness fluctuations of two monolayers.[16]

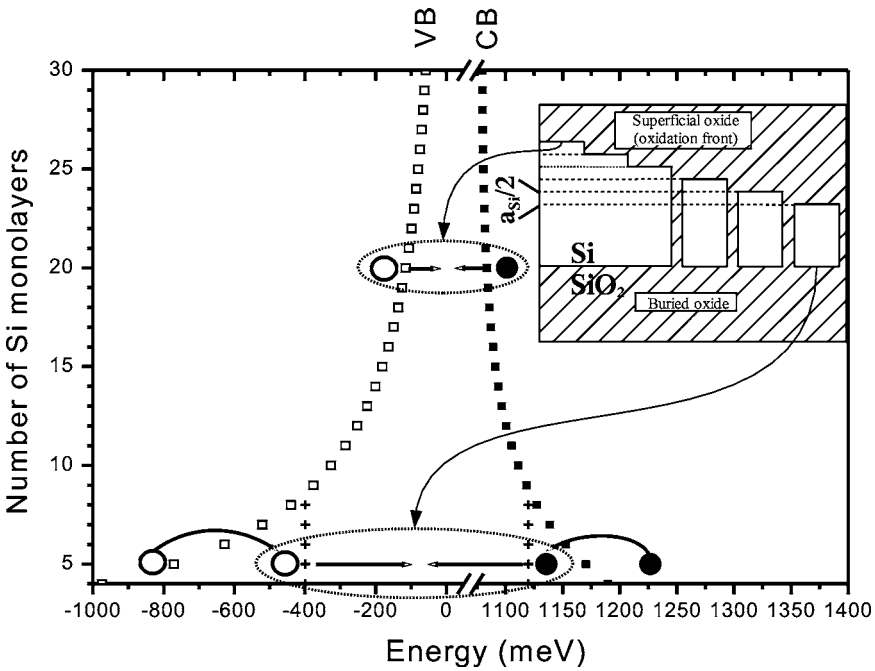

FIG. 4. Electronic processes at stake in narrow QW's in the scheme of band-to-band transitions (large thickness) and of activated carrier trapping on interfacial centers, assumed to be the Si and O atoms of the Si═O bonds, as deduced from Ref. 17 (small thickness). Inset: formation of the 2D nanoplates assembly for the thinnest QW's and corresponding band diagrams. The scale of length along the QW is contracted.

In view of the multicomponent nature of the PL spectra reported in Fig. 2 and of the previous conclusions, we deduce that the laser spot samples several l_z for a definite position.

As mentioned above, no luminescence contribution was found beyond E_{M5}. This result is *a priori* surprising in a scheme of quantum confinement since e-h recombination in a $\eta=6$ monolayer QW is expected to produce 1.78-eV photons (see Fig. 3). Such processes do not occur so that the 1.60-eV line seems to be the ultimate and more energetic PL line produced by *c*-Si QW's when the Si layer progressively vanishes.

Many authors reported the observation of this red PL line for narrow SIMOX QW's (Refs. 5–8) and a similar PL signal in porous silicon.[17] Thanks to a rigorous control of the QW thickness, we have shown in this work that the band edges continuously move from their bulk position up to very far values for the thinnest wells. Thus, the experimental freezing of e-h recombination at 1.60 eV is likely due to trapping of carriers on constant-energy levels. This kind of e-h recombination is activated when quantum confinement is sufficiently strong—i.e., when l_z passes below a critical value. For such a thickness, the conduction- and valence-band edges cross the trap levels so that the lower-energetic transitions are no longer the band-to-band recombination but recombination via trap levels. For Takahashi *et al.*,[6] excited carriers transfer and recombine on an interfacial trap when confinement is sufficiently strong. This assumption on the nature of the traps—i.e., of interfacial type—is supported by the experimental and theoretical work of Wolkin *et al.*[17] on the luminescence properties of *c*-Si nanocrystals (*nc*-Si) and the role of oxygen. As we did for *c*-Si QW's, they found a clear effect of the *nc*-Si size reduction on the PL properties, resulting in a blueshift of the e-h recombination line. This effect due to quantum confinement is seriously altered when *nc*-Si crystals are oxidized: the PL peak position of the smallest crystallites redshifts towards the same recombination energy. Their numerical calculations show that the Si═O bond creates interfacial traps while the band gap is opening due to quantum confinement in small crystallites, with activated trapping of one electron and one hole on the Si and O atoms, respectively.[17]

In view of the above-mentioned results, we assume that the 1.60-eV line is produced by e-h recombination on interfacial traps of very thin QW's, as reproduced in Fig. 4. *Ab initio* calculations of the electronic structure of nanometric *c*-Si QW's taking account of the great density of oxygen atoms and silicon oxygen bonds at the interface would be very useful to understand the physical processes at stake in such nanostructures.

B. Correlation between structure and light emission

In the previous section, we explained the multicomponent nature of the PL spectra in Figs. 2 and 3 as the result of quantized fluctuations of the QW thickness. The absence of thermalization between the different components indicates that carriers are strongly localized although they are *a priori* free to diffuse towards the deepest energetic well—i.e., the largest thickness—and to recombine to give a unique PL line.

A crude estimate of the maximum carrier mean free path before recombination $L_{e,h}$ can be made by equating the carrier velocity to the Fermi velocity v_F in the 4.7-nm QW (Ref. 10) ($v_F^{e,h} \approx 12\times 10^6$ cm s^{-1}). Assuming that the pair lifetime is of the order of 200 ns—as for EHL e-h pairs in a 28-nm QW (Ref. 10), we deduce that $L_{e,h} \approx 2.5$ cm, which is somewhat greater than the real carrier spreading radius $r_p \approx 500$ μm of an e-h plasma with $n \approx 3.2\times 10^{18}$ cm^{-3} and $\mathcal{P}=4\times 10^3$ W cm^{-2} in a 2-nm QW. These values indicate that e-h pairs should "explore" all the volume of the layer with various accessible l_z before they recombine. In the case of a thickness gradient with a gradual variation of the confinement energy, a driving force which attracts carriers from

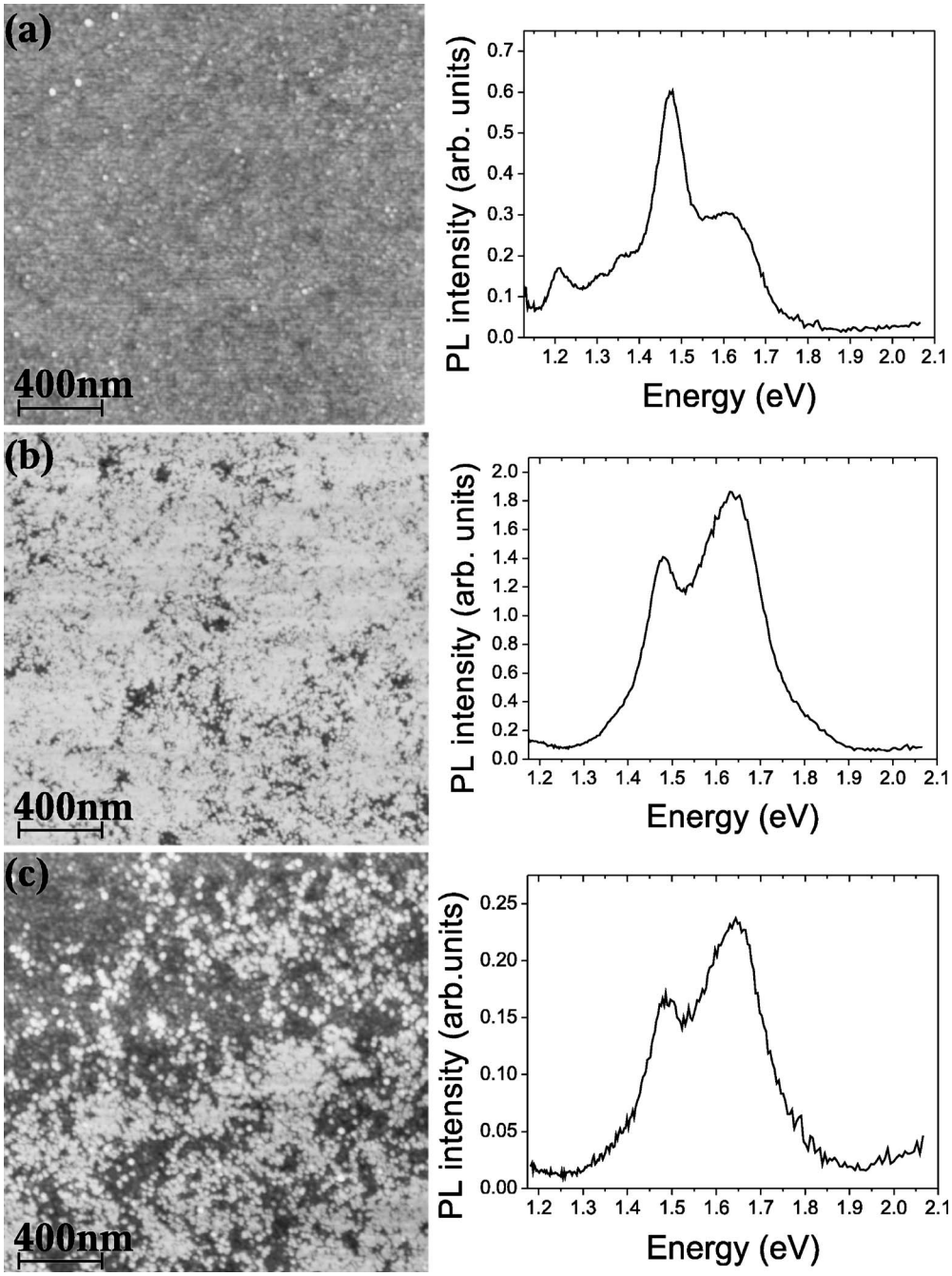

FIG. 5. AFM images of a QW surface (field=2 μm) obtained after removal of the top oxide. Images (a), (b), and (c) correspond to scanned zones with decreasing mean thickness. Bright surfaces are flat and are made of crystalline silicon, whereas the dark underlying surfaces correspond to SiO_2. The step between the Si and SiO_2 surfaces arising from the oxide etching is about 6 nm.

low to high l_z would result in an efficient e-h recombination in the lowest-energy state. A single line should be seen which is not the case in our samples—see Figs. 2 and 3. Then, we conclude that structural barriers for carrier motion form in the plane of the very narrow QW's, stop the carrier diffusion, and fix e-h transitions to the local value arising from the quantum confinement properties.

In order to determine the structure of narrow QW's, we performed a surface analysis of a sample coming from the edge of a wafer by atomic force microscopy (AFM), as shown in Fig. 5. Images (a), (b), and (c) have been recorded for decreasing mean thicknesses, after deoxidation of the top oxide in a buffered HF/NH_4F solution. In these pictures, *c*-Si is bright whereas the underlying oxide is dark. These data show a clear change in the surface state of the silicon layer when l_z is lowered from a few nanometers (a) down to a few monolayers (c). The QW surface, continuous and atomically flat (a), progressively breaks into a planar distribution of Si nanocrystals and/or two-dimensional Si grains, which we call nanoplates (c), lying on 6-nm SiO_2 pillars resulting from a low overetching of the buried oxide layer. Note that the buried oxide etching must be very well con-

trolled and limited to prevent the entire consumption of the oxide pillars and detachment of the upper dots. However, such a process is expected to remove the smallest crystallites from the sample surface and does not allow to exactly prepare the sample with its initial silicon surface state. Due to the radius of curvature of the AFM tip, the lack of lateral resolution prevents us from accurately measuring the diameter of the objects coming from the QW breaking. Thus, we cannot estimate the aspect ratio and the dimensionality of these dots. We conclude that data acquired via AFM corroborate the spectroscopic observation of various lines on the same PL spectrum and the model of blocked thermalization of carriers by structural barriers in ultrathin *c*-Si QW's. The inset in Fig. 5 gives a schematic view of the thickness gradient as deduced from spectroscopic and AFM measurements. According to Fig. 2, the QW surface is no longer continuous below the mean thickness $l_z \approx 2.1$ nm. In view of these results, the thermal thinning of SOI wafers down to $l_z \leqslant 2.1$ nm, in the "dot domain," appears as a promising way to make *c*-Si nanostructures particularly suitable for single-electron electronics.

Moreover, correlation between the QW surface structure and the light emission can be found by comparing cw PL spectra obtained before the top oxide deoxidation and AFM images, as reported in Fig. 5 (right column). The great rise in the intensity of the 1.60-eV line when the quantum dot density increases for the lowest thickness—Figs. 5(a)–5(c)—strongly suggests to us that the 1.60-eV contribution is ascribed to e-h recombination in Si dots. Complementary experiments would be necessary to observe the fine structure of luminescence spectra from single Si dots obtained using the thermal oxidation technique. Cathodoluminescence or confocal spectroscopy would be of great interest to determine the dependence of the trap level as a function of the nanoplate and nanocrystal diameters.

C. Quantum efficiency of *c*-Si QW's as a function of thickness

The previous study of PL spectra of thick and narrow QW's as a function of l_z brings other important information on the relation between carrier localization and the quantum efficiency (QE), defined as the e-h pair radiative recombination probability. In bulk *c*-Si, the usual value of $\mathrm{QE} \approx 1 \times 10^{-5}$ due to preeminence of Auger processes makes *c*-Si a bad candidate for applications in optoelectronics. Thinning *c*-Si QW's and localizing carriers to lower the probability of phonon-assisted e-h recombination appears as a practical way to rise the silicon QE. Here, we will use previous data to plot the $\mathrm{QE}(l_z)$ function and compare it with a simple model that takes account of the carrier localization in a 2D medium.

At first, it is useful to define the integrated intensity I_{int} of a given PL spectrum by the relation

$$I_{int} = \int_{h\nu_1}^{h\nu_2} \frac{S(h\nu)}{C(h\nu)} dh\nu, \tag{4}$$

where $h\nu_1$ and $h\nu_2$ are the lower and higher photon energies of the PL spectrum, S is the recorded signal by our lock-in amplifier system, and C is the setup response to the white lamp. A more practical physical parameter has to be introduced—namely, the photoluminescence efficiency η, defined as the integrated intensity per pump energy unit:

$$\eta(l_z) = \frac{I_{int}}{\mathcal{P} \times A(l_z)}, \tag{5}$$

$A(l_z)$ being the absorption coefficient at $\lambda = 351$ nm. Due to the lack of accurate knowledge in the absolute spectral sensitivity of the setup, it is very difficult to estimate the true value of the QE for a given QW. Here, a relative estimate of the PL efficiency gain with respect to the bulk value is much more convenient. We choose $\eta_{bulk} = I_{int}^{bulk}/\mathcal{P}[1 - A(3.9\ \mathrm{nm})]$ as the standard bulk value of the PL efficiency, where I_{int}^{bulk} is the integrated intensity of the substrate lines of the $l_z = 3.9$ nm QW as shown in Fig. 2 and $\mathcal{P} = 7 \times 10^3$ W cm^{-2}. Using the relation $\eta(l_z)/\eta_{bulk} = \mathrm{QE}(l_z)/\mathrm{QE}_{bulk}$ and previous spectroscopic data (cf. Fig. 2 and supplementary data not shown in this figure[10]), one obtains the thickness dependence of the relative gain in the quantum well QE, as reported in Fig. 6.

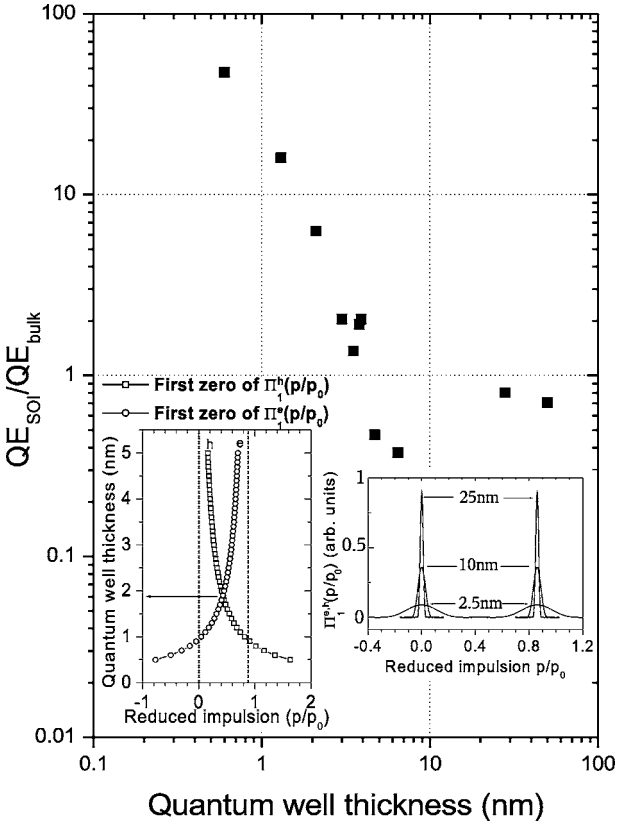

FIG. 6. Gain in the QW quantum efficiency with respect to substrate as a function of thickness. Inset: overlap of electron and hole wave functions. Right: probability $\Pi_1^{e,h}$ of finding an electron (respectively, a hole) in a $p_z = \hbar k_z$ state for various localization degrees. Left: edge positions of the $\Pi_1^{e,h}$ functions as a function of thickness in the first Brillouin zone, with $p_0 = \hbar 2\pi/a_{Si}$, impulsion at the edge of the first Brillouin zone.

The ratio $\mathrm{QE}(l_z)/\mathrm{QE}_{bulk}$ is almost constant and close to unity over a wide range of thickness provided that $l_z \geqslant 3$ nm. We conclude that the SOI QE remains unchanged, as the result of the constancy of phonon-assisted e-h processes down to $l_z \approx 3$ nm and the very low density of nonra-

diative recombination centers in these, artificial structures.

Below $l_z \approx 3$ nm, the quantum efficiency gains until two decades for the thinnest QW's, in qualitative agreement with the expected increase of the no-phonon-assisted e-h recombination due to the spreading in the **k** space of the carrier wave functions. If we keep in mind the AFM pictures of the QW surface shown in Fig. 5, the actual values of $\mathrm{QE}(l_z)/\mathrm{QE}_{bulk}$ in the thinnest QW's should be seriously reevaluated since the covering rate of the silicon layer is not 100%. This results in a lowering of the PL-integrated intensity and in an artificial underestimate of the PL efficiency compared to the case of a total covering by quantum dots.

In our high-potential-barrier QW's, the wave functions associated with the e-h stationary states is written $\Phi_n^{e,h}(z) = \sqrt{2/l_z}\sin[n\pi z/l_z]$ along the z direction ($n=1$ corresponding to the ground state). Localizing the carriers in the (x,y) plane leads to a broadening of the probability functions $\Pi_1^{e,h}(p_z) = |\langle \Phi_1^{e,h} | k_z \rangle|^2$ of finding an electron (respectively, a hole) in a $p_z = \hbar k_z$ state given by

$$\Pi_1^{e,h}(p_z) = \left\{ \frac{1}{2i}\sqrt{\frac{l_z}{\pi\hbar}}\exp\left[i\left(\frac{\pi}{2} - \frac{p_z l_z}{2\hbar}\right)\right] \times \left[F\left(p_z - \frac{\pi\hbar}{l_z}\right) + F\left(p_z + \frac{\pi\hbar}{l_z}\right)\right]\right\}^2, \quad (6)$$

where $F(p_z) = \sin[p_z l_z/2\hbar]/(p_z l_z/2\hbar)$. In the case of crystalline silicon and to simply account for the effect of localization, we shall center the $\Pi_1^h(p_z)$ function at the Γ point and $\Pi_1^e(p_z)$ function at the $\mathbf{k} = [\pm 0.86, 0, 0]2\pi/a_{Si}$ point on the electronic band diagram of silicon—this latter point corresponds to the position of the conduction-band minimum in the ΓX direction.

The right inset in Fig. 6 gives a schematic view of the spreading phenomenon of the wave functions of an electron and a hole under strong localization and clearly shows that no overlap occurs for large thickness between the e-h probability functions. The left inset reports a plot of the first right and left zeros of the $\Pi_1^h(p_z)$ [$\Pi_1^e(p_z)$, respectively] functions when centered on the valence- and conduction-band edges, respectively. Appreciable overlap is found below $l_z \approx 1.9$ nm, which can explain the significant increase in the QE in narrow QW's as a result of direct recombination via highly confined states. Here, the mass of carriers has no influence on the form of the probability functions and then any change in the band curvature arising from a decrease in the QW thickness has no effect on the result of the calculations.

According to the results of the preceding section, this "localization" model can be hardly compared to spectroscopic data acquired on the thinnest nanostructures since no uniform silicon layer with mean thickness $l_z \leqslant 2.1$ nm can form. This model agrees well with our experimental data in the sense that no noticeable increase in the QE is observed in QW's with $l_z \geqslant 3$ nm. Fabrication of a set of ultrathin SOI wafers with *uniform* and monolayer-defined silicon layers would be of great interest to test the relevance of our approach. Moreover, data analysis reveals that the change in the slope of the $\mathrm{QE}(l_z)$ curve below $l_z \approx 3$ nm is mainly ascribed to the 1.46-eV e-h recombination and the so-called 1.60-eV interfacial transitions. This particular transition via trap levels needs a more specific treatment and does not obey our previous model. AFM surface analyses (see Fig. 5) tend to prove that recombination on interfacial traps only occurs in *nc*-Si-type structures (i.e., silicon dots) and that the adequate approach to describe e-h processes in those structures should be done by means of *ab initio* calculations, as Delerue *et al.* did for porous silicon.[2]

In their theory, the calculated recombination rate of e-h pairs in silicon crystallites is found to be of radiative type when the diameter d is sufficiently small due to direct recombination and increases when d decreases. In addition, if the diameter of the nanostructures is smaller than the mean distance between the nonradiative recombination centers, an extra contribution term due to the spatial confinement effect contributes in the QE increase. A theoretical study of the influence of the carrier localization on the Si═O bonds on the e-h pairs recombination dynamics would be very interesting to compare with our data.

IV. CONCLUSION

In this article, the transition between two-dimensional and zero-dimensional $\mathrm{Si/SiO_2}$ nanostructures is observed. The quantum confinement effect involves important line blueshifts, up to 600 meV with respect to bulk samples. For the thinnest wells, the discrete series of high-energy PL lines reveals that carrier energy levels are also discrete. A simple model based both on the thickness dependence of the band gap and on the e-h interactions in the QW has been presented to account for these results and connects these electronic states to monolayer-defined regions of the sample. The experimental freezing of the QW luminescence at 1.60 eV is ascribed to e-h recombination via localized states on the Si═O bond of the $\mathrm{Si/SiO_2}$ interface. Supplementary experiments such as thermal treatments in controlled atmospheres should be performed to break the Si═O bonds and to observe the expected quenching of the 1.60 eV line and extra-high-energy PL lines originating from highly confined electronic states.

ACKNOWLEDGMENTS

We would like to thank V. Salvador and J. L. Rouvière from CEA-Grenoble for preparation and observation of TEM samples.

*Present address: Université de Sherbrooke, Département de génie électrique et génie informatique, 2500 boulevard de l'université, J1K 2R1, Sherbrooke, Québec, Canada. Electronic address: nicolas.pauc@usherbrooke.ca

†Electronic address: calvo@drfmc.ceng.cea.fr

[1] N. G. Way Lek, M. A. Lourenço, R. M. Gwilliam, S. Ledain, G. Shao, and K. P. Homewood, Nature (London) **410**, 192 (2001).

[2] C. Delerue, G. Allan, and M. Lannoo, Phys. Rev. B **48**, 11024 (1993).

[3] L. T. Canham, Appl. Phys. Lett. **57**, 1046 (1990).

[4] F. Mazen, T. Baron, A. M. Papon, R. Truche, and J. M. Hartmann, Appl. Surf. Sci. **214**, 359 (2003).

[5] P. N. Saeta and A. C. Gallagher, Phys. Rev. B **55**, 4563 (1997).

[6] Y. Takahashi, T. Furuta, Y. Ono, and T. Ishiyama, Jpn. J. Appl. Phys., Part 1 **34**, 950 (1995).

[7] S. Okamoto and Y. Kanemitsu, Solid State Commun. **103**, 573 (1997).

[8] M. Y. Kanemitsu and T. Kushida, J. Lumin. **87-89**, 463 (2000).

[9] Y. Wang, Y. Ishikawa, and N. Shibata, Jpn. J. Appl. Phys., Part 1 **41**, 5177 (2002).

[10] N. Pauc, V. Calvo, J. Eymery, F. Fournel, and N. Magnea, Phys. Rev. Lett. **92**, 236802 (2004).

[11] T. M. Rice, J. C. Hensel, T. G. Phillips, and G. A. Thomas, in *Solid State Physics*, edited by H. Ehrenreich, F. Seitz, and D. Turnbull (Academic Press, New York, 1977), Vol. 32.

[12] Here, we use "e-h recombination line" instead of "EHL recombination line" because we do not know the exact nature of the e-h phase in very thin QW's.

[13] Y. M. Niquet, C. Delerue, G. Allan, and M. Lannoo, Phys. Rev. B **62**, 5109 (2000).

[14] D. A. Kleinman, Phys. Rev. B **33**, 2540 (1986).

[15] L. Keldysh, Phys. Status Solidi A **164**, 3 (1997).

[16] It has been shown by scanning reflection electron microscopy (SREM) that the Si(001) surface oxidation occurs layer by layer (Ref. 18). The atomic step at the interface did not move laterally and step-flow propagation with step bunching is not observed during the oxidation mechanism of standard silicon (001) surface. In this paper, the PL method gives information about the total thickness of the SOI film. The observation of the bilayer distribution in the Si film thickness results probably from the morphology of the initial film. But the thickness fluctuation—and the two-Si-surface correlation—is not well studied in the literature. The present optical experiments suggest that these correlations should be analyzed in details, for example, with transmission electron microscopy for very small SOI thickness to understand the miscut, thickness, temperature role on the coupling between the two surfaces. This point is clearly not in the scope of this paper, but is clearly interesting for future work.

[17] M. V. Wolkin, J. Jorne, P. M. Fauchet, G. Allan, and C. Delerue, Phys. Rev. Lett. **82**, 197 (1999).

[18] H. Watanabe, K. Kato, T. Uda, K. Fujita, M. Ichikawa, T. Kawamura, and K. Terakura, Phys. Rev. Lett. **80**, 345 (1998).